AD-A187 416 MBE (MOLECULAR BEAM EPITAXIAL) GROWTH CHARACTERIZATION AND ELECTRONIC DEV.. (U) CHICAGO UNIV ILL DEPT OF PHYSICS J FAURIE 15 JUN 87 AFOSR-TR-87-1629 1/1

UNCLASSIFIED F49620-87-C-0021 F/G 20/2 NL

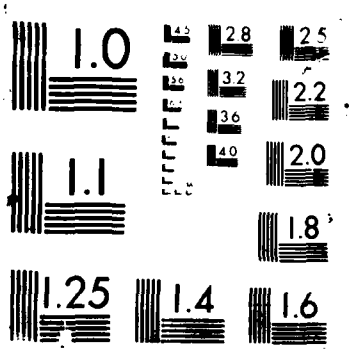
1.0
1.1
1.25
1.4
1.6
1.8
2.0
2.2
2.5
2.8
3.2
3.6
4.0

UNCLASSIFIED
SECURITY C

(2)

DOCUMENTATION PAGE

1a. REPOR UNCLASS	1b. RESTRICTIVE MARKINGS
2a. SECURI UNCLASSIFIED	3. DISTRIBUTION/AVAILABILITY OF REPORT Approved for public release; distribution unlimited.
2b. DECLASSIFICATION/DOWNGRA SCHEDULE N/A	
4. PERFORMING ORGANIZATION REPORT NUMBER(S)	5. MONITORING ORGANIZATION REPORT NUMBER(S) AFOSR-TR-87-1629
6a. NAME OF PERFORMING ORGANIZATION University of IL, Chicago Department of Physics	6b. OFFICE SYMBOL (If applicable)
6c. ADDRESS (City, State and ZIP Code) Chicago, Illinois 60680	7a. NAME OF MONITORING ORGANIZATION Same as 8a
	7b. ADDRESS (City, State and ZIP Code) Same as 8b
8a. NAME OF FUNDING/SPONSORING ORGANIZATION AFOSR	8b. OFFICE SYMBOL (If applicable) NE
	9. PROCUREMENT INSTRUMENT IDENTIFICATION NUMBER F49620-87-C-0021
8c. ADDRESS (City, State and ZIP Code) Bldg 410 Bolling AFB, DC 20332-6448	10. SOURCE OF FUNDING NOS.

PROGRAM ELEMENT NO.	PROJECT NO.	TASK NO.	WORK UNIT NO
61102F	DARPA		

11. TITLE (Include Security Classification) MBE Growth Characterization & Electronic Device Processing of HqCdTe, HgZnTe, Related Heterojunctions and HgCdTe-CdTe Superlattices

12. PERSONAL AUTHOR(S) Jean-Pierre Faurie

13a. TYPE OF REPORT	13b. TIME COVERED	14. DATE OF REPORT (Yr., Mo., Day)	15. PAGE COUNT
QUARTERLY	FROM 6/15/87 TO _____	87/06/15	24

16. SUPPLEMENTARY NOTATION

17. COSATI CODES			18. SUBJECT TERMS (Continue on reverse if necessary and identify by block number)
FIELD	GROUP	SUB. GR	

19. ABSTRACT (Continue on reverse if necessary and identify by block number)

As the MBE growth technique has continued to improve for Hg(1-x)Cd(x)Te films, the prospects for films of larger area have begun to be explored. These larger area films are important for imaging arrays and will be especially vital in the future for the efficient production of Hg(1-x)Cd(x)Te material. The growth of MBE of uniform Hg(1-x)Cd(x)Te epilayer on a large substrate is very difficult to achieve because of the non-uniform distribution of the fluxes and on the non-uniform temperature of the substrate. .

20. DISTRIBUTION/AVAILABILITY OF ABSTRACT	21. ABSTRACT SECURITY CLASSIFICATION
UNCLASSIFIED/UNLIMITED ☒ SAME AS RPT ☐ DTIC USERS ☐	UNCLASSIFIED

22a. NAME OF RESPONSIBLE INDIVIDUAL	22b. TELEPHONE NUMBER (Include Area Code)	22c. OFFICE SYMBOL
JEAN-PIERRE FAURIE	(312) 996-3400	

DD FORM 1473, 83 APR EDITION OF 1 JAN 73 IS OBSOLETE

UNCLASSIFIED
SECURITY CLASSIFICATION OF THIS PAGE

MBE GROWTH, CHARACTERIZATION AND ELECTRONIC DEVICE PROCESSING OF HgCdTe, HgZnTe, RELATED HETEROJUNCTIONS AND HgCdTe-CdTe SUPERLATTICES

DARPA - AFOSR - F49620-87-C-0021
November 13, 1986 - November 12, 1989

Quarterly Report
June 15, 1987

Jean-Pierre Faurie
University of Illinois at Chicago

I. MBE growth and Characterization of two-inch diameter p-type $Hg_{1-x}Cd_xTe$ films on GaAs (100) substrate.

As the Molecular Beam Epitaxial (MBE) growth technique has continued to improve for $Hg_{1-x}Cd_xTe$ films, the prospects for films of larger area have begun to be explored. These larger area films are important for imaging arrays and will be especially vital in the future for the efficient production of $Hg_{1-x}Cd_xTe$ material. The growth by MBE of uniform $Hg_{1-x}Cd_xTe$ epilayer on a large substrate is very difficult to achieve because of the non-uniform distribution of the fluxes and on the non-uniform temperature of the substrate.

But above all, the main problem is due to the exponential change of the Hg condensation coefficient with temperature. We have shown that for a given Hg flux, a high quality monocrystalline $Hg_{1-x}Cd_xTe$ film can be grown in the (111)B orientation within a narrow substrate temperature range (T_{max}-T_{min}) of about 10-15 C° if the substrate temperature (T_s) is in the 180-190°C temperature range. When T_s is lower than T_{min} the Hg in excess desorbs but twins, detrimental for the electrical performance, are observed. When T_s is above T_{max} two possibilities exist. If T_s is below 190 C° the Te in excess leads to a polycrystalline material. If T_s is above 195 C° the excess of Te is reevaporated and the film still grows monocrystalline, but an increase in the x-value of about 1.5 to 2% for each 1°C increase in the substrate temperature is observed along with a large change in the growth rate.

It is important to recall that a change in Δx of only ± 0.001 is the objective suitable to reach for infrared photovoltaic detectors operating with a cutoff wavelength of 10μm at 77K. It is obvious that such a requirement cannot be achieved if part of the substrate is above T_{max}. Now if the substrate temperature is between T_{max} and T_{min} (incidentally T_{max} and T_{min} values are changing over the substrate since the Hg flux distribution is not constant) the epilayers will still experience a change in the doping level and even in the conduction type.

To minimize these temperature variations the rotation of the substrate during the growth can help but a precise temperature measurement of the substrate by a thermocouple is hindered. In order to have an adequate control of the temperature during the growth which can also give reproducible results an infrared pyrometer has been used.

The combination of flux distribution and substrate temperature variation makes the growth by MBE of a large, high quality and uniform $Hg_{1-x}Cd_xTe$ film to be a real challenge.

The film presented here was grown in the (111)B orientation. The film exhibits a uniform mirror-like surface. In order to ascertain the uniformity of this $Hg_{1-x}Cd_xTe$ films over its two-inch diameter surface area, infrared transmission and Van der Pauw D.C. Hall measurements were performed at several positions. The infrared transmission spectra were measured at room temperature. The cutoff wavelengths were in the 6 to 8 μm region. The cutoff wavelength is defined as that for which the absorption coefficient α is equal to 500 cm^{-1}, where the formula for the absorption coefficient is α = -ℓn (transmittance)/thickness. From the measured cutoff wavelengths for each position on the two-inch diameter $Hg_{1-x}Cd_xTe$ films, the Cd concentrations (x) were calculated using Hansen et al.'s relation[7]. Also, from the interference spacing in the infrared transmission spectrum the thicknesses at these positions on the film were determined.

For the p-type film reported here the uniformity of the x-value proved to be excellent, as illustrated in figure 1. The average value of x (denoted by $\bar{x}$) was 0.22, while the standard deviation $\Delta x = [\Sigma(x-\bar{x})^2/n-1]^{1/2}$ was 0.0015, giving as a measure of the composition uniformity $\Delta x/x = 0.7\%$. This is an excellent result since the goal required for IR detectors in terms of composition uniformity is almost achieved on this two-inch diameter $Hg_{1-x}Cd_xTe$ film. This film is entirely p-type. Carrier concentrations (N_a-N_d) and Hall mobilities are reported in Table 1. N_a-N_d increased by a factor of two from 2.6×10^{15} cm^{-3} at the edge of the film, while μ_H increased from 5.7×10^2 $cm^2V^{-1}s^{-1}$ at the center to 6.2×10^2 $cm^2V^{-1}s^{-1}$ at the edge.

These variations are supposed to be due to a non uniform flux distribution and a non uniform substrate temperature. A ΔT_s of about 5°C has been measured over 2 inches.

This result represents an important achievement for the future of IR detectors. As an important comparison this result is as good as those reported for OMCVD HgCdTe films grown on a surface area of only [x]cm^2.

$Hg_{1-x}Cd_xTe$ (111)B grown on 2° GaAs(100)–Sample #583453

T_s = 195 °C

Thickness = 5.4 μm

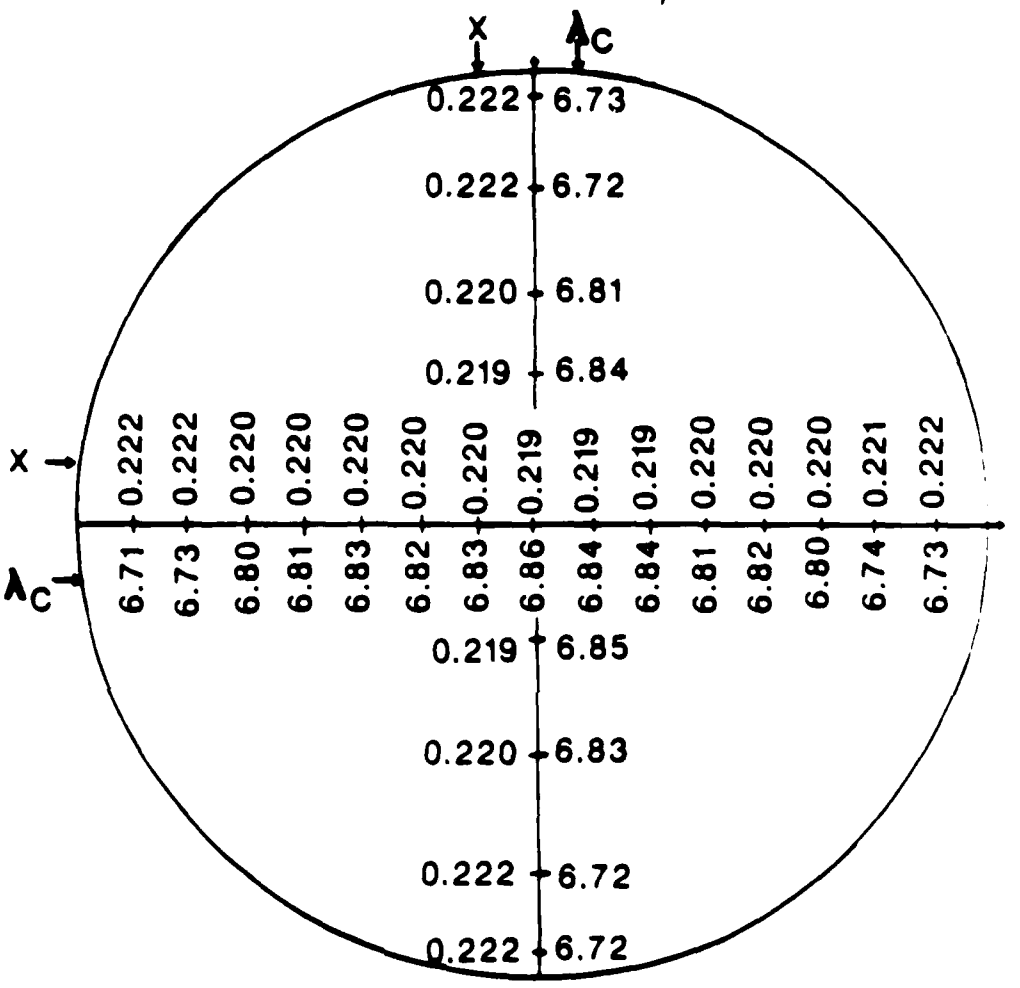

λ = cut-off wavelength in μm at 300K

$\bar{x}$ = 0.22 $\qquad$ $\bar{\lambda}$ = 6.78 μm

$$\Delta x_{SD} = \sqrt{\frac{\Sigma(x-\bar{x})^2}{n-1}} = 0.0015 \qquad \Delta\lambda_{SD} = 0.08\ \mu m$$

$$\frac{\Delta x_{SD}}{\bar{x}} = 0.7\ \%$$

Table I - Hall measurements at B = 0.2 Tesla for two-inch diameter $Hg_{1-x}Cd_xTe(111)$ film grown at 190°C on CdTe(111)/GaAs(100) substrate. Sample #583453.x=0, y=0 is at the center of the sample.

x (mm)	y (mm)	Cond. Type	300K N_d-N_a (cm^{-3})	μ_H ($cm^2V^{-1}s^{-1}$)	T(K) when $R_H=0$	Cond. Type	40K N_a-N_d (cm^{-3})	μ_H ($cm^2V^{-1}s^{-1}$)
0	0	n	2.1×10^{16}	6.4×10^{3}	90	p	3.6×10^{15}	5.7×10^{2}
4	0	n	2.0×10^{16}	5.0×10^{3}	90	p	3.0×10^{15}	5.2×10^{2}
7	0	n	2.1×10^{16}	6.3×10^{3}	90	p	4.7×10^{15}	5.5×10^{2}
11	0	n	1.9×10^{16}	6.2×10^{3}	90	p	5.1×10^{15}	5.7×10^{2}
15	0	n	1.9×10^{16}	6.8×10^{3}	90	p	5.6×10^{15}	6.5×10^{2}
18	0	n	1.8×10^{16}	6.8×10^{3}	90	p	7.2×10^{15}	6.2×10^{2}
0	7	n	1.9×10^{16}	6.6×10^{3}	90	p	4.9×10^{15}	6.0×10^{2}
0	15	n	1.8×10^{16}	6.8×10^{3}	90	p	6.1×10^{15}	6.7×10^{2}

II. P-TYPE DOPING

In the previous report (March 15, 1987) it has been shown that under regular MBE growth conditions As and Sb are incorporated as donors in HgCdTe. Therefore in order to obtain p-type HgCdTe layers incorporation of a Group I element was studied.

Lithium was the first element investigated. It is found that Li is indeed incorporated as an acceptor. Acceptor concentrations as high as $8\times10^{8}cm^{-3}$ have been achieved. An incorporation coefficient of Li close to one and almost a 100% electrical efficiency for Li were observed in Li-doped $Hg_{1-x}Cd_xTe$ epilayers grown by MBE without any external activation. However, Li is found to diffuse rapidly in MBE HgCdTe grown layers.

For more detail see the attached paper submitted to Applied Physics Letters entitled "Electrical Properties of Li Doped $Hg_{1-x}Cd_xTe(100)$ by Molecular Beam Epitaxy".

III. HgTe-CdTe Superlattices: Hg incorporation in CdTe layers during MBE growth

It was shown in 1982 that HgTe-CdTe superlattices (SLs) could be grown by MBE. But due to the noncongruent evaporation of Hg from HgTe, the Hg flux must be maintained even during the growth of the CdTe layers. This means that some Hg is incorporated in the CdTe during its growth. There are two important questions that arise. First, how will this Hg incorporation affect the bandgap of the SL. Second, how much Hg is in the CdTe.

We determine the period of the SL by the position of the X-ray satellite peaks. The average Hg composition in the SL is then measured by EDS. The period and the average Hg composition are then used to compute the individual layer thicknesses if the percentage of Hg in the CdTe is known. Using this method, for the same period and average Hg composition, as the amount of Hg in the CdTe increases several things will occur. First, the thickness of the HgTe layers will decrease. This will tend to increase the bandgap. Second, the CdTe will become $Hg_xCd_{1-x}Te$ with a smaller bandgap. This decrease in the barrier height will tend to decrease the SL bandgap. Finally, the width of the Hg_xCd_{1-}

$_x$Te will increase. This will have a small tendency to increase the bandgap. The total effect on the SL bandgap of all these changes would be small.

We have grown, with a Hg flux, thick layers of CdTe under the same conditions as in our SLs [190 to 200°C on (111)B]. The amount of Hg measured in the layer by EDS was less than 5%. On a series of thin CdTe (111)B layers grown under a Hg flux the amount of Hg was carefully measured by XPS. This is done using both the ratio of the peak areas and the difference in energy between the core level and valence band maximum. For the growth conditions that we actually use in our SLs, these results agree with those obtained for the thick layers. The Hg incorporation varies, up to 9%, depending on the growth conditions. This should only slightly affect the characteristics of the HgTe-CdTe SLs and other micr-ostructures, such as single and double barrier tunneling structures.

These results indicate that some Hg is incorporated in the CdTe but that under our normal conditions this amount is small. The Hg incorporation is crystal orientation dependent. For the (100) surfaces, about 15% Hg are observed for growth conditions identical to those used for the (111).

For more information see the attached paper accepted for publication in Applied Physics Letters (Nov. 1987) entitled "Hg Icorporation in CdTe Dring the Gowth of HgTe-CdTe Sperlattices by Molecular Beam Epitaxy."

FILE: 023745APL 381 QUEUE:APL-APL
IS: pasteup FMT: aipxr
BY: REV: JOYCE ;02/10,19:22
03-OCT-87 11:26:27

TABLE I. Hg to Te ratio in CdTe grown with a Hg flux on CdTe substrates, along with the growth conditions. T_s is the substrate temperature. The CdTe growth rate was held constant at about 1 Å/s.

Substrate orientation	T_s (°C)	Hg flux (10^{17} cm^{-2} s^{-1})	$1-x$ (area ratios)	$1-x$ (binding energies)
(111)*B*	175	1.6	0.085 ± 0.009	0.087 ± 0.020
(111)*B*	185	1.6	0.065 ± 0.015	0.051 ± 0.020
(111)*B*	195	1.6	0.057 ± 0.016	···
(111)*B*	195	0.89	0.045 ± 0.010	0.070 ± 0.020
(111)*B*	195	1.6	0.057 ± 0.016	···
(111)*B*	195	2.2	0.085 ± 0.016	0.100 ± 0.020
(100)	185	1.6	0.147 ± 0.016	···

TABLE II. Hg to Te ratio in CdTe grown with a Hg flux along with the growth conditions. All were grown on a CdTe (111)*B* buffer layer but the initial substrate was varied. T_s is the substrate temperature. Estimated Hg flux: 1.6×10^{17} cm^{-2} s^{-1}.

Substrate	T_s (°C)	CdTe growth rate (Å/s)	$1-x$ (area ratios)	$1-x$ (binding energies)
CdTe	195	0.5	0.030 ± 0.004	0.043 ± 0.020
CdTe	195	1.0	0.057 ± 0.016	···
CdTe	195	2.0	0.078 ± 0.008	···
GaAs	185	1.0	0.065 ± 0.007	0.043 ± 0.020
GaAs	195	1.0	0.036 ± 0.008	···

023745APL = 023745APL
Running Title:

Hg incorporation in CdTe during the growth of HgTe-CdTe superlattices by molecular beam epitaxy

J. Reno,[a] R. Sporken,[b] Y. J. Kim, C. Hsu, and J. P. Faurie
Department of Physics, University of Illinois at Chicago, Chicago, Illinois 60680

(Received 3 August 1987; accepted for publication 9 September 1987)

HgTe-CdTe superlattices and other microstructures such as single and double barrier tunneling structures are commonly grown by molecular beam epitaxy with the mercury flux continuously on the sample during the growth. This means that some mercury will be incorporated in the CdTe layers. We present here, for the first time, a measurement of the amount of mercury incorporated in thin layers of CdTe. X-ray photoelectron spectroscopy was used to measure the amount of mercury. The amount of mercury was found to be between 3 and 9% for CdTe (111)*B*, depending on the growth conditions. The amount of mercury was found to increase with mercury flux and to decrease as the substrate temperature was increased. Under the same conditions, it was found that much more mercury was incorporated in the (100) orientation. The type of substrate (CdTe or GaAs) was not found to influence the results. These results indicate that the amount of mercury in the CdTe layers of HgTe-CdTe superlattices is not quite as low as expected from measurements of thick CdTe layers, but it can be low enough that it does not influence significantly the results on the superlattice system in the (111) orientation.

HgTe-CdTe superlattices have been proposed as a new, interesting infrared material.[1,2] It has been shown that they can be grown by molecular beam epitaxy (MBE).[3] It has also been shown that the best growth temperature is 180–200 °C.[3] At this temperature the mercury condensation coefficient is about 10^{-3}.[4] This means that a large mercury overpressure is needed to grow HgTe. It also implies that mercury will easily and noncongruently evaporate from HgTe. Due to this problem, the common growth technique for HgTe-CdTe superlattices and other microstructures such as single and double barrier tunneling structures involves leaving the Hg source open at all times.[5,6] Thus, there is a mercury flux on the sample during the growth of the CdTe layers. A competition then occurs between the Hg and Cd atoms for lattice sites. As a result, the CdTe layers may not be pure CdTe but instead be $Hg_{1-x}Cd_xTe$ with some percentage of mercury.

This problem was recognized by the first people to grow HgTe-CdTe superlattices on CdTe (111)*B* substrates. They grew thick layers of CdTe under the same conditions as in the superlattice, including the presence of the Hg flux. The Hg content was then measured by energy dispersive spectroscopy (EDS). It was found that the CdTe contained less than 5% mercury.[7] When we began to grow HgTe-CdTe superlattices at the University of Illinois, we repeated these experiments with the same results.[5] This small amount of mercury should only slightly influence the characteristics of the superlattices such as the band gap and the valence-band discontinuity. Therefore, it was neglected. The only question was whether the results for a thick layer were the same for the thin layer in the superlattice.

Recently, it has been suggested that the amount of mercury in the CdTe layers of the superlattice might not be as small as previously thought.[8] For this reason we have performed the first measurements of the amount of mercury incorporated in *thin* CdTe layers grown with a mercury flux. We have also looked at how the amount of mercury incorporated depends upon the substrate temperature, the mercury flux, the CdTe growth rate, and on the type and orientation of the substrate.

The samples were all grown at the University of Illinois in a Riber 2300 MBE machine. CdTe substrates oriented in the (100) and the (111)*B* were used. Additionally, GaAs(100) with both (100) and (111)*B* CdTe buffer layers were used. The substrate preparation and the growth of the appropriate buffer layer have been discussed elsewhere.[5] The Te flux was kept constant throughout the experiment. The flux was chosen so that the HgTe growth rate was about 5 Å/s on a CdTe(111)*B* substrate. A CdTe growth rate of 1 Å/s was used throughout the experiment, except when that growth rate was the parameter being varied. These growth rates are typical of those used in the growth of HgTe-CdTe superlattices. The substrate temperature was measured using a chromel-alumel thermocouple in contact with the sample holder and by an infrared pyrometer. These measurements have been calibrated using the melting temperatures of indium and tin.

The structure of the samples was chosen to be similar to that of the superlattices. On the buffer layer a HgTe layer with a thickness of 80–100 Å was grown first. This was immediately followed by a CdTe layer 150–170 Å thick. The CdTe layer was grown with the Hg flux still on the sample.

The Hg concentration in the CdTe layers was measured by x-ray photoelectron spectroscopy (XPS) using both the ratio of peak areas and the energy difference between the Hg 5*d* or Cd 4*d* core level and the valence-band maximum (VBM). For $Hg_{1-x}Cd_xTe$, this energy difference can be shown to reflect the position of the VBM on an absolute energy scale, because the cation core levels are virtually independent on the alloy composition x.[9,10] The position of the VBM is known in turn to be very sensitive to the composition x.[9,10] Therefore, the binding energy of the Hg 5*d* and Cd 4*d* core levels with respect to the VBM can be used to determine the alloy composition x. Several samples were grown without the HgTe layer on the bottom to see if its presence changed the measurement. No difference was found in the Hg concentration in the CdTe whether the HgTe was present or not. First with the Te and CdTe fluxes constant, the substrate temperature and the Hg flux were varied to determine their influence on the Hg incorporation.

The samples were kept under ultrahigh vacuum conditions as they were transferred to the XPS chamber. The XPS measurements were performed with an SSX-100 spectrometer from Surface Science Laboratories. A monochromatized and focused Al $K\alpha$ excitation line was used. The overall energy resolution measured on the Au $4f_{7/2}$ core level is 0.7 eV. The core levels used in this work were the Hg 4*f* and 5*d*, the Cd 4*d* and 3*d*, and the Te 4*d* and 3*d*. The values of the peak areas and positions of all the core levels were determined by a detailed analysis of the spectra by a least-squares fit of individual spin-orbit doublets to the data. The line shape used for the fits was a Lorentzian convoluted with a Gaussian. A nonlinear background was subtracted from the spectra prior to the fitting procedure.

Figure 1 shows a typical result for the spectrum of the Cd 4*d* and the Hg 5*d* core levels. This is the most difficult case due to the large number of overlapping peaks. The fit reveals the existence of two Hg components. These two components will be called $Hg^{(1)}$ and $Hg^{(2)}$ in the following discussion. From its binding energy with respect to the VBM,[10] $Hg^{(1)}$ can be clearly identified as Hg in $Hg_{1-x}Cd_xTe$. The origin of $Hg^{(2)}$, at about 600 meV higher binding energy, is not yet fully understood. We believe that $Hg^{(2)}$ is some sort of surface mercury. Further experiments are still in progress to clarify this point. Only the component $Hg^{(1)}$, associated with Hg in $Hg_{1-x}Cd_xTe$, was used in our measurements. It is the only one that should influence the band gap, if $Hg^{(2)}$ is indeed a surface phenomenon.

To obtain the binding energies ($E_{Cl} - E_v$) used for the determination of the Hg concentration, the position of the VBM was determined simply by a linear extrapolation of the valence-band leading edge. This procedure has proven to be reproducible and very accurate for Te-based II-VI semiconductors.[11] Since the binding energy defined above is very sensitive to the Hg concentration in $Hg_{1-x}Cd_xTe$,[10] it can be used to determine the amount of Hg in the CdTe. As can be seen in Table I, there is good agreement between the two methods. This gives us confidence in our results and in neglecting the $Hg^{(2)}$ component. This procedure implies the measurement of the valence-band energy distribution curve and is thus highly time consuming. Therefore, it was not applied systematically to all the samples.

In order to compare our previous results for a thick layer with these for a thin layer, we grew a thick CdTe layer and checked the Hg concentration with both XPS and EDS. The growth conditions were similar to those used for the thin layers (T_s = 195 °C, Hg flux = 1.6×10^{17} $cm^{-2}s^{-1}$, and CdTe growth rate 1 Å s^{-1}). The results from EDS agreed with all of our earlier work and gave a value of about 3% Hg in the CdTe. The XPS results on this layer gave a Hg concentration of 5%. This difference is within the range of experimental error, but it may also indicate that there is a slight difference in the Hg concentration with depth.

The homogeneity of the Hg distribution with depth can be checked by comparing results from core levels at different binding energies. In our case the determinations using the Hg 4*f*, Cd 3*d*, and Te 3*d* core levels are more surface sensitive than those using the Hg 5*d*, Cd 4*d*, and Te 4*d* lines. This is due to the smaller escape depth for the Cd 3*d* and Te 3*d* photoelectrons ($\lambda \simeq 15$ Å) compared to the Cd 4*d* and Te 4*d* ($\lambda \simeq 20$ Å). We found that the more surface-sensitive determinations systematically yielded slightly higher concentrations. Compared with EDS, XPS is primarily a surface technique. The observed surface enrichment is thus consistent with the difference between the bulk results from EDS and the XPS results. Further investigations with good depth resolution would certainly be very desirable to confirm (or inform) this point.

Table I summarizes the Hg concentrations determined by XPS for the different substrate and Hg cell temperatures. The Hg concentrations determined by both XPS methods are given. The values given in the table based on peak area ratios are average values from four different sets of core level spectra. Relative sensitivity factors were determined for our instrument from MBE grown HgTe (111) and CdTe (111) samples.

The Hg flux was determined using Knudsen's effusion law, which is a good approximation in this case for the direction normal to the evaporating surface. A change of the substrate temperature by 10 °C will change the Hg condensation coefficient by about a factor of 1.5.[4] Several striking features are observed from this table. First, for these growth conditions on CdTe (111)*B* the amount of Hg incorporated is much less than 20%.[12] Second, the overall agreement between the area ratio and the binding energy results is good. Third, the amount of Hg incorporated follows the general trends expected from the growth conditions, and the relative magnitudes are in reasonable agreement with the Hg flux and condensation coefficient variations. Fourth, a Hg concentration of 5% was obtained by the correct selection of the growth conditions and we have obtained a value as low as 3% in a second set of experiments.

It has been reported that for a CdTe (211) substrate the amount of Hg incorporated is about 20%.[13] We have also shown that the Hg condensation coefficient varies depending on the orientation of the substrate.[4] For this reason, we have also investigated CdTe (100). The fluxes were the same as used for the (111)*B*. The results are also given in Table I. The difference in the Hg incorporation is very large and opposite to our initial expectations, since Hg on CdTe (100) has the smaller condensation coefficient of these two orientations. We do not understand these results, but they show once again that MBE growth cannot be treated by a classical thermodynamic approach using the law of mass action and neglecting surface kinetics.

We performed a second set of experiments to check the dependence of the Hg incorporation on the CdTe growth rate and on the type of substrate. The Te and Hg fluxes were kept constant. The results are given in Table II.

The first point that can be seen from these results is that it does not matter whether a CdTe (111)*B* substrate or a GaAs (100) substrate with a CdTe (111)*B* buffer is used to grow the layers. The Hg incorporation is about the same for the two different substrates. The second point is that the Hg incorporation appears to increase with the CdTe growth rate. We do not have much data, but the trend appears to be in this direction.

It was also found that the quality of the surface prior to the growth of our structures could dramatically influence the amount of Hg incorporated. If the same substrate was reused frequently and thus re-etched several times or an inadequate buffer layer was grown, a significantly larger Hg incorporation was found. This means that extreme care must be taken not only when doing this type of experiment but also when preparing a substrate on which to grow a superlattice.

In conclusion, we have presented for the first time a measurement of the amount of mercury incorporated in thin layers of CdTe grown under mercury flux. The growth conditions and the structures were chosen to be similar to those in HgTe-CdTe superlattices. When carefully prepared, layers grown on CdTe (111)*B* were found to contain between 3 and 9% mercury. The amount of mercury was found to increase with the mercury flux and the CdTe growth rate, and to decrease as the substrate temperature was increased. We did not observe any significant dependence of the amount of mercury incorporated on the type of substrate but there was a large dependence on the orientation of the substrate. We found that much more mercury was incorporated for (100) than for (111)*B* prepared under the same conditions. We thus expect the Hg incorporation in CdTe (100) to be even more important under normal growth conditions.[14] This dependence of the amount of mercury incorporated on the growth conditions and the substrate orientation means that care must be taken when comparing results between different groups. Also, dramatic increases in the amount of Hg incorporated can occur if the initial surface is not properly prepared. These results indicate that the amount of mercury incorporated into carefully prepared (111)*B* superlattices is small enough that it should not significantly influence the characteristics of the superlattices previously reported, and in particular the value of the valence-band discontinuity and the band gaps.

This work carried out at the University of Illinois at Chicago was supported by the Defense Advanced Research Projects Agency and monitored by the Air Force Office of Scientific Research under contract No. F4920-87-C-0021. One of us (R. S.) is supported in part by the National Belgian Foundation for Scientific Research (FNRS).

[a] Present address: Sandia National Laboratory, Organization 1144, Albuquerque, NM 87185.
[b] Permanent address: Facultes Universitaires Notre-Dame de la Paix, B-5000 Namur, Belgium.

[1] J. N. Schulman and T. C. McGill, Appl. Phys. Lett. **34**, 663 (1979).
[2] D. L. Smith, T. C. McGill, and J. N. Schulman, Appl. Phys. Lett. **43**, 180 (1983).
[3] J. P. Faurie, A. Million, and J. Piaguet, Appl. Phys. Lett. **41**, 713 (1982).
[4] J. P. Faurie, A. Million, R. Boch, and J. L. Tissot, J. Vac. Sci. Technol. A **1**, 1593 (1983).
[5] J. P. Faurie, IEEE J. Quantum Electron. **QE-22**, 1656 (1986).
[6] K. A. Harris, S. Hwang, D. K. Blanks, J. W. Cook, J. F. Schetzina, N. Otsuka, J. P. Baukus, and A. T. Hunter, Appl. Phys. Lett. **48**, 396 (1986).
[7] J. P. Faurie, A. Million, and J. Piaguet (unpublished results, 1982).
[8] S. Perkowitz, D. Rajavel, I. K. Sou, J. Reno, J. P. Faurie, C. E. Jones, T. Casselman, K. A. Harris, J. W. Cook, and J. F. Schetzina, Appl. Phys. Lett. **49**, 806 (1986).
[9] C. K. Shih and W. E. Spicer, Phys. Rev. Lett. **58**, 2594 (1987).
[10] C. Hsu, T. M. Duc, and J. P. Faurie (unpublished).
[11] T. M. Duc, C. Hsu, and J. P. Faurie, Phys. Rev. Lett. **58**, 1127 (1987).
[12] S. Perkowitz, R. Sudharsanan, [redacted], and S. S. Yom, J. Vac. Sci. Technol. ~~(to be published)~~.
[13] M. W. Goodwin, M. A. Kinch, R. J. Koestner, M. C. Chen, D. G. Seiler, and R. J. Justice, J. Vac. Sci. Technol. ~~(to be published)~~.
[14] S. Sivananthan, X. Chu, J. Reno, and J. P. Faurie, J. Appl. Phys. **60**, 1359 (1986).

FIG. 1. Typical XPS spectrum from a CdTe layer grown with a mercury flux. The dash-dotted line is the result of a least-squares fit to the data. The dashed lines represent the individual components used for this fit. The background is represented by the solid line. The dots are the experimental data.

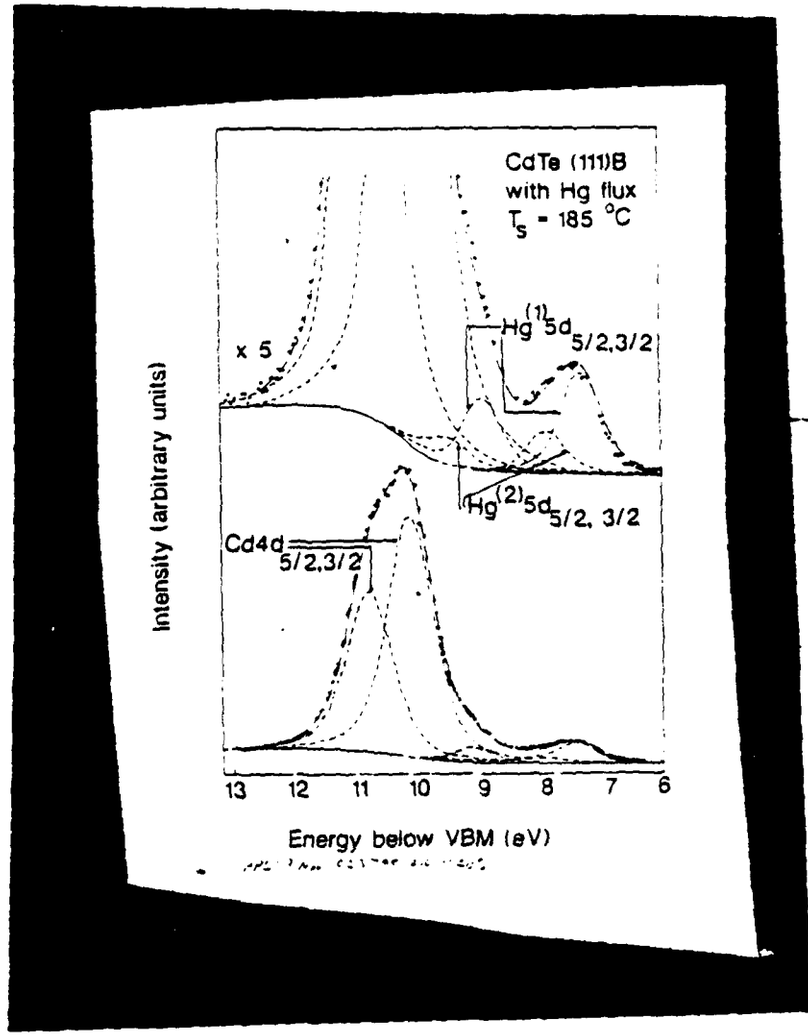
CdTe (111)B
with Hg flux
T_s = 185 °C
x 5
$Hg^{(1)}5d_{5/2,3/2}$
$Hg^{(2)}5d_{5/2,3/2}$
$Cd4d_{5/2,3/2}$
Intensity (arbitrary units)
13
12
11
10
9
8
7
6
Energy below VBM (eV)

Applied Physics Letters (Submitted)

Electrical Properties Of Li Doped $Hg_{1-z}Cd_zTe$(100) By Molecular Beam Epitaxy

P.S.Wijewarnasuriya, I.K.Sou, Y.J.Kim, K.K.Mahavadi,
S.Sivananthan, M.Boukerche and J.P.Faurie

Dept. of Physics, University of Illinois at Chicago, Chicago,Il. 60680

Abstract

P-type doping of HgCdTe(100) layers with lithium during growth by molecular beam epitaxy is reported. Hall measurements have been performed on these layers between 300K and 30K. The Li concentration is found to increase with the Li cell temperature. Li doped HgCdTe layers are estimated to have very shallow acceptor levels. Acceptor concentrations as high as 8×10^{18} cm^{-3} have been achieved. At low doping levels, due to residual donors, layers show compensation. Incorporation coefficient of Li close to one and almost 100% electrical efficiency for Li in molecular beam epitaxy HgCdTe layers were observed. However, Li is found to diffuse rapidly in HgCdTe layers grown by molecular beam epitaxy.

Over the past ten years $Hg_{1-x}Cd_xTe$ (MCT) has emerged as an important material for infrared(IR) detector technology. MCT was grown by Molecular Beam Epitaxy (MBE) on CdTe substrates for the first time in 1981.[1] Since then, this technique has produced MCT layers of either n or p type and of a quality comparable to the layers grown by other techniques. However, very little information exists on the incorporation of foreign elements in MBE grown epitaxial layers. Recently, successful n-type doping of MCT layers with indium during growth by MBE was reported.[2] Carrier concentrations of two orders of magnitude more than what can be achieved by stoichiometry deviation have been reached for MBE layers grown in the (111)B orientation. Antimony and arsenic (group V elements) act as p-type dopants in MCT using other growth techniques[3] such as liquid phase epitaxy. But in the case of MBE grown MCT layers, both Sb and As behave as a n-type dopants.[4] In the case of (100) orientation only n-type MCT with doping levels ranging from 10^{15} to mid-10^{16} cm^{-3} can easily be produced by stoichiometry deviation for $x<0.35$. P-type (100) is difficult to achieve for $x<0.24$.[5] Therefore, in order to obtain p-type MCT layers in the (100) orientation, incorporation of foreign elements in group I was studied. Li behaves as a p-type dopant, as expected. Here, we report results on Li, the first impurity successfully incorporated as an electrically active acceptor in MBE-grown MCT layers.[4] In this letter, we present electrical properties of lithium-doped MCT(100) MBE layers studied by variable temperature Hall measurements.

MCT layers were grown in a Riber 2300 MBE machine which is designed to handle mercury. MCT layers were grown on 2-3 μm thick CdTe buffer layer which was deposited on GaAs(100) substrates. The growth was monitored by reflection high energy electron diffraction(RHEED). The growth rate was 4-5 Å/Sec. Li was provided by a separated effusion cell loaded with pure Li. Since it is a very reactive material, great care has been taken when loading it into the growth chamber. This was done in an inert atmosphere. The Li cell temper-

ature range was from 205°C to 280°C. The Cd composition in the MCT layers was determined at room temperature by infrared transmission measurements and by energy dispersive spectroscopy measurements. The secondary ion mass spectroscopy (SIMS) technique was used to obtain the concentration profile of Li atoms through the layers. Since we did not have a standard sample containing Li, we were not able to relate the number of counts from the SIMS to the actual Li concentration. Therefore, all SIMS data are given in arbitary units, but a relative comparison is significant. The carrier concentration and the Hall mobility in the layers were evaluated by the Van der Pauw technique[6] between room temperature and 30K. An $AuCl_3$ solution was used to form ohmic contacts, and the ohmicity of the contacts was checked systematically. A magnetic field strength of 2000 Gauss was used for the Hall measurements.

Electrical measurements of the Li doped MCT layers at 40K are summarized in Table I. Figure 1 shows the variation of the carrier concentration (deduced from the Hall coefficient) vs 1000/T(K) for three samples. A typical freeze-out behaviour cannot be seen for the larger doping levels. This happens even with mid 10^{17} doping levels and above. Such an effect has been reported previously for phosphorous.[7] Furthermore, it can be seen from the figure that the mixed conduction N⇒P transition region diminishes when the doping level increases. For the higher doping levels, the carrier concentration is independent of temperature, indicating that electrically active acceptors are completly ionized. The total amount of electrically active Li concentration in the samples was determined from the low temperature carrier concentration data.

The only layer (sample #1) which shows the freeze-out behaviour has been analyzed numerically[8] using the charge neutrality equation:

$$n + N_a^- = p + N_d^+$$

where n,p,N_d^+ and N_a^- are the concentration of electrons, holes, ionized donors

and ionized acceptors, respectively. For the donors, complete ionization is assumed and the concentration of ionized acceptors is given by

$$N_a^- = \frac{N_a}{1 + 4 * exp(x_a - \eta_f)}$$

where x_a is the reduced acceptor level with respect to valence band ; η_f is the reduced Fermi level.

From the Kane model[9] for nonparabolic bands, n is

$$n = \frac{K_B T}{2\pi^2}\left(\frac{3}{2P^2}\right)^{3/2} \int_0^{+\infty} \frac{x^{1/2}(x + x_g)^{1/2}(2x + x_g)}{1 + exp(x + x_g - \eta_f)}\, dx.$$

Where P is the momentum matrix element of the Kane model and x_g is the reduced energy gap. For the band gap E_g, an empirical equation is used from Ref. 10. Since the equilibrium concentration of light hole is negligible, p is the heavy-hole concentration. Parabolic band with Fermi-Dirac statistics is assumed for the heavy holes. Since the mixed conduction dominates at high temperature, the concentration is deduced from the following equation:

$$C.C. = \frac{(p + nb)^2}{(p - nb^2)}$$

where b is the ratio of electron-to-hole mobility and is given by

$$b = \frac{\mu_e}{\mu_h} = \tau \times \frac{m_h^*}{m_e^*}$$

where $m_e^* = 3\frac{\hbar^2 E_g}{4P^2}$, $m_h^* = .63 \times m_e^{(11)}$ and $P = 8 \times 10^{-8}$ ev cm[11]

When calculating, N_a,N_d,τ and E_a were adjusted to give the best fit for the experimental carrier concentration data. The solid line in Fig.1 is the best fit. It was obtained with $N_a = 1.89 \times 10^{16}$ cm^{-3}, $N_d = 1.05 \times 10^{16}$ cm^{-3}, $\tau = .24$, $E_a = 8.3$meV and Cd composition=25.8%

Figure 2 shows mobility vs doping concentration at 40K. It can be seen that the hole mobility in the Li doped samples at 40K does not vary drastically with the hole concentration. Doping levels as high as $8\times10^{18}cm^{-3}$ were achieved. At low doping levels, experimental results indicate a large degree of compensation in the layers, since along the (100) growth orientation, only n-type MBE grown MCT(100) layers are currently achieved by stochiometry adjustment. (see Table 1). This large degree of compensation accounts for the limitation of the hole mobility at low doping levels.

Fig. 3 shows the concentration of Li atoms in the MCT layers calculated from the incident flux and from growth rate (assuming unity sticking coefficient) vs 1000/T(K), where T is the Li cell temperature. The carrier concentration N_a-N_d (extracted from Hall measurements) and the SIMS Li counts are also plotted in Fig. 3. By comparing the concentration of electrically active Li atoms in the layers from Hall measurements and the concentration of Li atoms incorporated into layers calculated from the incident flux, it can be seen that there is good agreement within the experimental error. At this range of doping levels, N_a-N_d extracted from Hall measurements is approximately equal to the acceptor concentration N_a, since residual donor concentration is of the order of $10^{16}cm^{-3}$. Therefore, this agrement is an indication that almost 100% of the Li is electrically efficient, and also that the incorporation of Li in MBE grown MCT layers is close to one. As can be seen from Fig. 3, the SIMS data falls on a straight line, indicating that the number of Li atom incorporated into the samples decreases exponentially with the reciprocal of the Li cell temperature. Sample #1, which has the lowest Li cell temperature, exhibits a large discrepancy between Li concentration as calculated from the incident flux and as measured from Hall measurements. This discrepancy is due to the compensation in the layers because the level of electrically active impurities(Li) is not much larger than the intrinsic donors.

In order to investigate the diffusivity of Li, a sample consisting of a non-doped MCT layer(0.93μm thick) on top of a Li doped MCT layer(0.93μm thick) has been grown. From the SIMS profile of this sample, Li can be seen in the undoped layer in amounts comparable to that in the intentionally doped one. This indicates that Li is highly mobile in MCT layers grown by MBE. At this point, we have no evidence from SIMS data that Li is diffusing in CdTe buffer layer and substrate.

In conclusion, we have demonstrated that Li behaves as a p-type dopant in MBE grown $Hg_{1-z}Cd_zTe(100)$. This represents the first successful attempt to incorporate electrically active acceptors during MBE growth. These Li doped MCT layers have been estimated to have very shallow acceptor levels for sample #1, which showed the freeze-out. The calculated activation energy was 8.3mev. Using Li as a p-type dopant, carrier concentrations up to 8×10^{18} cm^{-3} have been achieved. At low doping levels, layers show compensation due to the residual donors from stoichiometry deviation. The doping level in the samples can be controlled by varying the Li cell temperature. An incorporation coefficient of one and almost 100% electrical efficiency for Li in MBE grown MCT layers were observed. However, the SIMS profile indicates that Li is highly mobile in MCT layers. This represents a limitation in the use of this element, especially for abrupt hetorojunctions.

We wish to acknowledge G. Monfroy for performing the energy dispersive spectroscopy measurements for some of the samples, and Z. Ali and A. Farook for their technical assistance. This work was funded by the Defense Advanced Research Project Agency and monitored by the Air Force Office for Scientific Research under contract No. F49620-87-C-0021

References:

1). J.P.Faurie and A.Million, *J. Cryst. Growth* **54**,582(1981).

2). M.Boukerche, J.Reno, I.K.Sou, C.Hsu and J.P.Faurie, *Appl. Phys. Lett.* **48**,1733(1986).

3). P.Capper, *J. Cryst. Growth* **57**,280(1982).

4). J.P.Faurie, *DARPA II-VI Materials & Processing Conference, Washinton, April 1987. (unpublished results)*

5). J.M.Arias, S.H.Shin, J.T.Chen, S.Sivananthan, J.Reno and J.P.Faurie, *J. Vac. Sci. Technol.* Sept.-Oct. 87 (in press)

6). L.J. van der Pauw, *Philips Tech. Rev.*, **20**,220(1958).

7). H.R.Vydyanth, R.C. Abbot and D.A. NElson,*J. Appl. Phys.* **54**, 1323(1983)

8). M.Boukerche, P.S.Wijewarnasuriya, J.Reno, I.K. Sou and J.P. Faurie, *J. Vac. Sci. Technol.* **A4(4)**,2072(1986).

9). E.O.Kane, *J.Phys.Chem.Solids* **1**,249(1957).

10). E.Finkman and S.E.Schacham, *J. Appl. Phys.* **56**,2896(1984).

11). E.Finkman, *J.Appl.Phys* **54**,1883(1983).

Table I. Electrical measurements of lithium doped MCT at 40K.
Sample # 6 and # 7 represents n-type MBE grown MCT(100).

Sample #	*Thickness* μm	*Cd composition* %	*Na-Nd* cm^{-3} $\times 10^{16}$	*Mobility* $cm^2/v.s$ *at 40K*	*Li cell Temp.* $^\circ C$
1	1.68	25	+0.84	370	205
2	1.38	17	+52.00	360	219
3	2.16	20	+200.00	330	245
4	2.18	23	+800.00	330	282
5	1.92	21	+440.00	340	270
6	1.00	20	-1.00	3.0×10^5	
7	6.20	19	-1.00	2.4×10^5	

Figure Captions

Fig.1: Hole concentration as a function of 1000/T(K) for lithium doped MCT layers grown by MBE. The solid line for sample #1 is the best fit obtained for the following parameters: N_a=1.89×10^{16},N_d= 1.05×10^{16},τ=.24 and E_a=8.3meV.

Fig.2: Experimental hole mobility at 40K as a function of the hole concentration for lithium doped MCT layers.

Fig.3: Li counts (◇)obtained by SIMS in the layers, N_a-N_d(cm^{-3}) from Hall measurements (□) and Li concentration(cm^{-3}) calculated from the incident flux (△) vs reciprocal of the Li cell temperature.

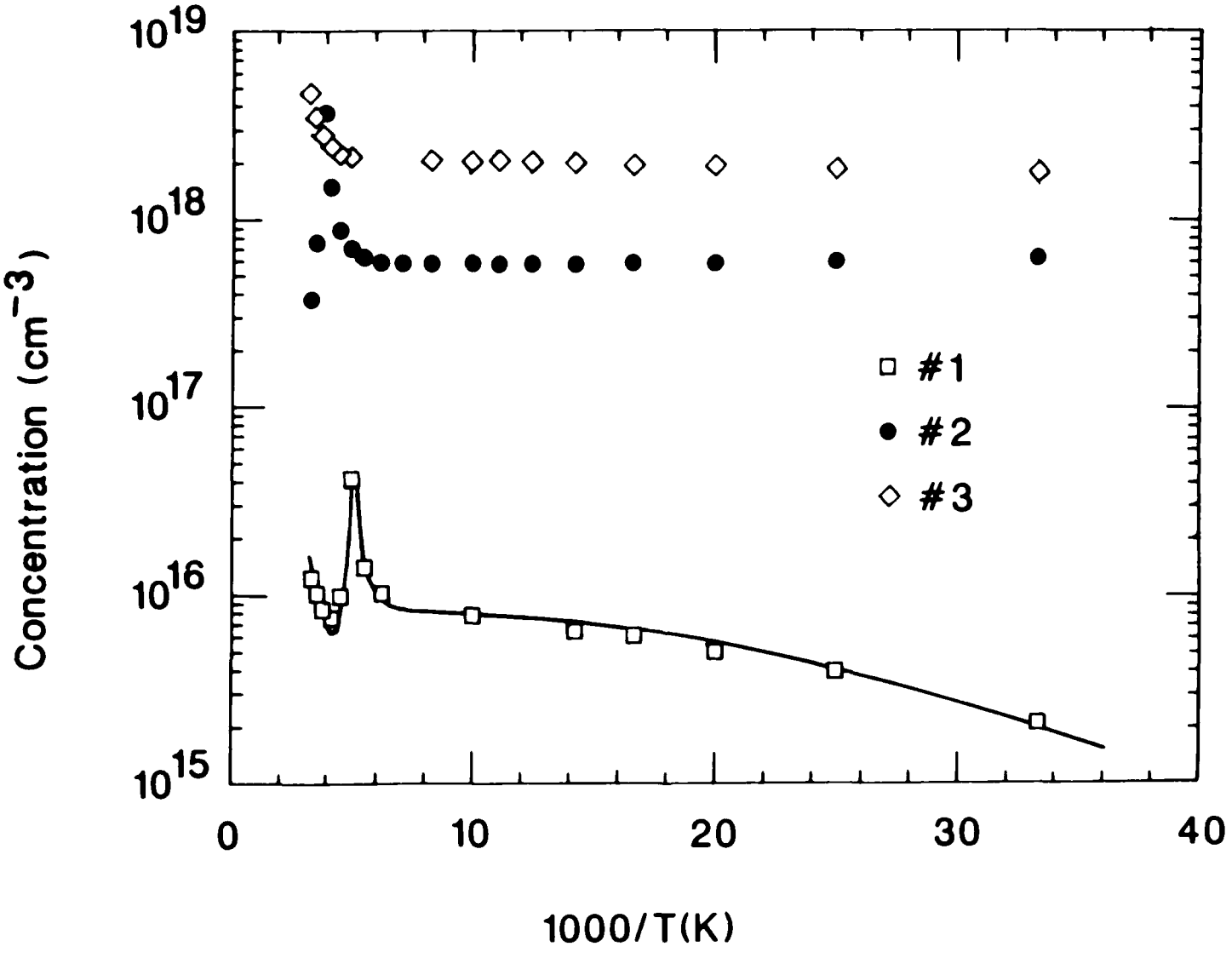
Concentration (cm^{-3})
10^{19}
10^{18}
10^{17}
10^{16}
10^{15}
0
10
20
30
40
1000/T(K)
#1
#2
#3

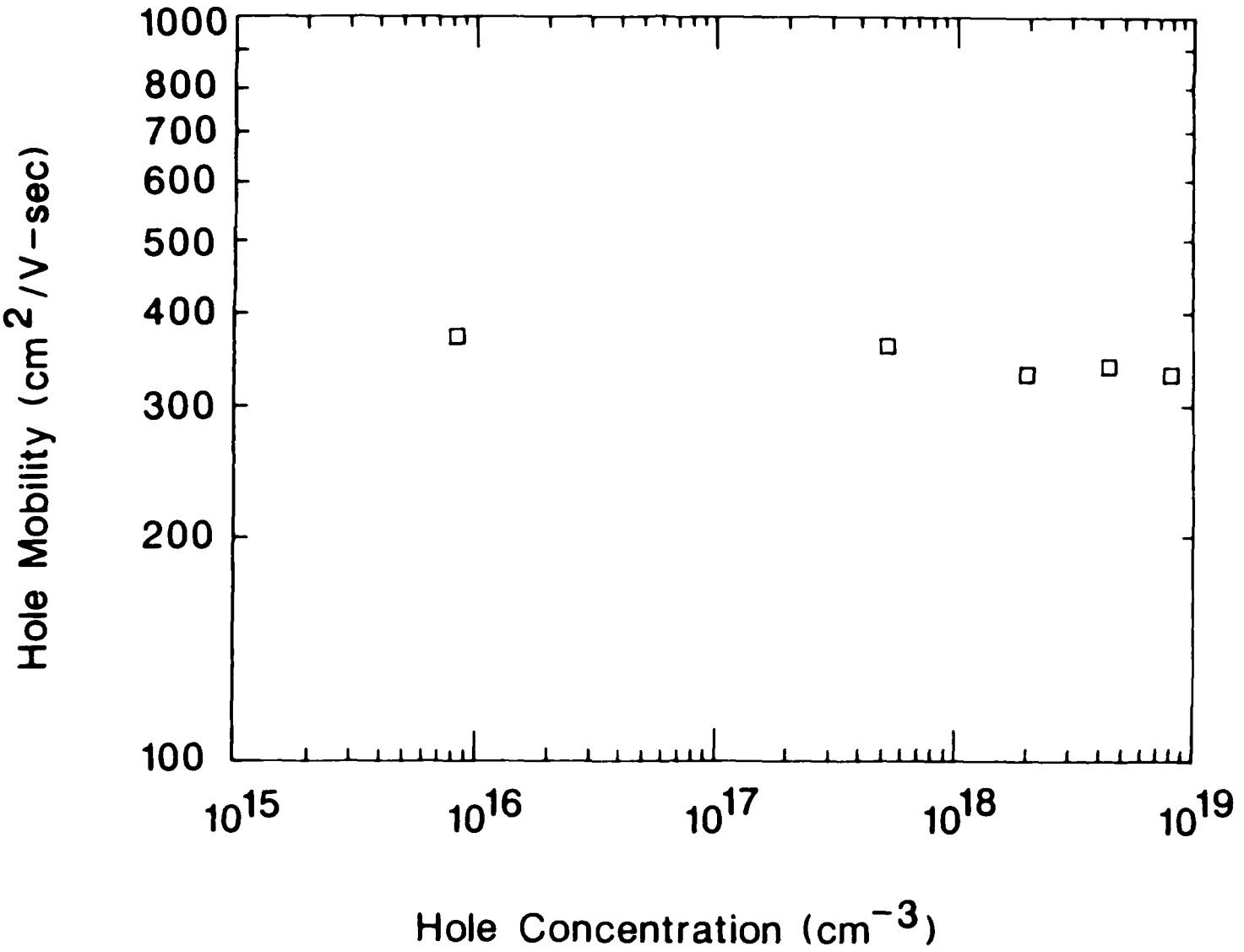
1000
800
700
600
500
400
300
200
100
Hole Mobility (cm^2/V-sec)
10^{15}
10^{16}
10^{17}
10^{18}
10^{19}
Hole Concentration (cm^{-3})

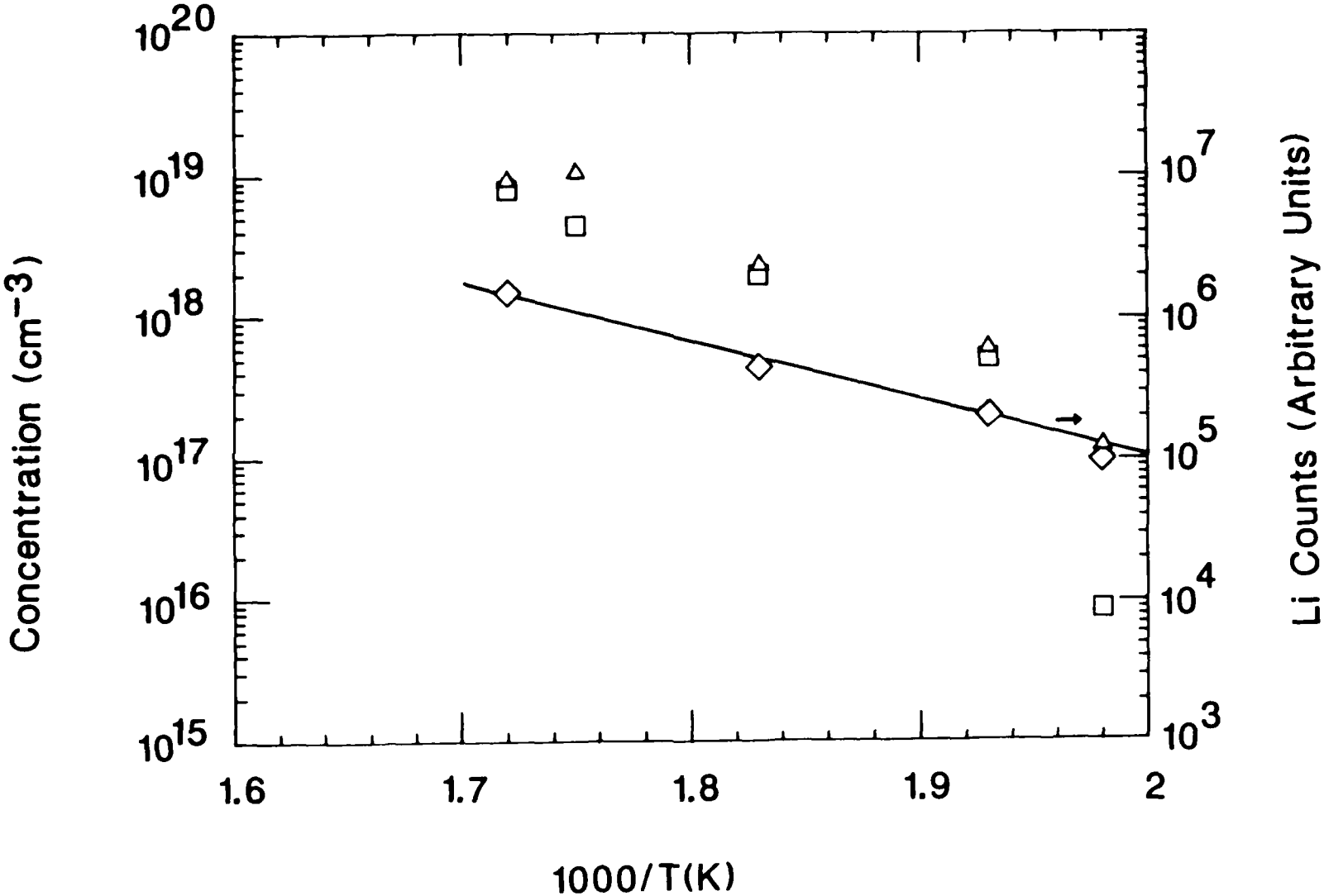
Concentration (cm^{-3})
10^{20}
10^{19}
10^{18}
10^{17}
10^{16}
10^{15}
10^{7}
10^{6}
10^{5}
10^{4}
10^{3}
Li Counts (Arbitrary Units)
1.6
1.7
1.8
1.9
2
1000/T(K)

END

DATE

FILMED

FEB.

1988